Table VIII. Summary of Proximity Analyses[a]

atom	1° coord no. reactants	t.s.	product	solute-water energy[b] reactants	t.s.	product
C	0.13	0	0	-0.5	0	0
H	1.95	1.14	1.27	-4.0	-4.8	-6.9
H	1.23	1.61	1.55	-2.0	-7.9	-3.9
O=	0.80	2.59	3.01	-2.5	-10.4	-14.2
O—	4.71	2.03	1.73	-21.0	-15.8	-10.4
H_O	0.79	0.50	1.04	-11.8	-7.8	-10.6
total	9.79	7.87	8.60			
1° energy contrib				-122.7	-81.1	-86.8
E_{sx}				-221	-151	-154
% contrib of 1° energy				56%	54%	56%

[a] Results from the three fixed-solute simulations. Cutoffs for each atom are C, 5.35 Å; H_C 3.00 Å; O=, 3.20 Å; O—, 3.20 Å; H_O 2.55 Å. [b] Average solute-water interaction energy (kcal/mol) for water molecules in the 1° coordination shell of the given atom.

reveal the origin of the activation barrier in solution. Specifically, the 5.5 strong interactions for OH^- become five or six weaker ones for the transition state and product. This reflects hydrogen bond weakening upon charge delocalization as noted above for the monohydrated complexes (Figures 3 and 4).

The quantitative impact of this effect is indicated by the contributions to the total solute-water interaction energies, E_{sx}, from the waters in the primary hydration shells. As listed in Table VIII, these contributions are -123, -81, and -87 kcal/mol for the reactants, transition state, and product. The difference of 42 kcal/mol between the reactants and transition state is undoubtedly the principal component of the hydration-induced barrier to the addition reaction.

Stereoplots. In closing, four stereoplots representing the last Monte Carlo configuration for the product, the transition state, and the reactants in both trajectories are shown in Figure 13. For clarity, water molecules more than 3 Å in front of the solutes have been removed. These plots illustrate many of the structural ideas discussed above.

For the reactants, the stereoplots clearly show the hydroxide ion participating in about 6 hydrogen bonds with one hydrogen of each water molecule pointing toward the hydroxide oxygen. The formaldehyde sits more in a solvent cavity with about 1 hydrogen bonded water molecule on the carbonyl oxygen. At the transition state, both oxygens of the solute appear to be participating in 3 hydrogen bonds. The density of water molecules around the transformed carbonyl oxygen increases in continuing to the product, though the total number of solute-water hydrogen bonds appears to remain constant at 6-7. In all of the plots except perhaps for the product, it does not appear that the hydroxide hydrogen in participating as a hydrogen bond donor. This seems reasonable, though not obvious a priori, for a relatively small anion on the electrostatic grounds discussed above. It should be remembered that these stereoplots show only one of millions of configurations that were sampled in the Monte Carlo calculations.

Conclusions

Through the use of quantum and statistical mechanical methods, a comprehensive examination of a nucleophilic addition in the gas phase and in aqueous solution has been carried out. The reaction of $OH^- + H_2C{=}O$ in the gas phase was found to have a shallow ion-dipole minimum along the lowest energy path to the tetrahedral intermediate. Upon hydration, a ca. 25 kcal/mol free energy barrier is introduced; the transition state was located at a CO separation of 2.05 Å. These results and the overall free energy change in water are consistent with prior experimental studies of hydrolysis reactions and with the theoretical results of Weiner et al. for the addition of hydroxide to formamide in water.[5,9,24] Further confirmation of these findings is possible through application of integral equation methods now that the necessary potential functions have been reported here.[30] There are a number of potential sources of error in the present study that should be kept in mind, including the choice and form of the intermolecular potential functions and the lack of intramolecular vibrations. Also, only two trajectories for the reaction in water could be studied since even this required the equivalent of ca. 300 days of VAX 11/780 time. Nevertheless, the present work and the earlier studies of an S_N2 reaction[8] represent a significant advance in the theoretical treament of organic reactions in solution. Both studies have yielded not only reasonable energetic results but also detailed insight into the change in solvation along the reaction paths. In particular, a general observation appears to be emerging for these polar reactions: it is not so much the change in number of hydrogen bonds along the reaction paths but rather in their strengths that is primarily responsible for the solvent-induced activation barriers.

Acknowledgment. Gratitude is expressed to the National Science Foundation for support of this work.

(30) Chiles, R. A.; Rossky, P. J. *J. Am. Chem. Soc.* **1984**, *106*, 6867.

Chemisorption Patterns as Predicted by Band Calculations, by Frontier Crystal Orbitals, and by Cluster Calculations: Hydrogen Atoms on Graphite

John P. LaFemina and John P. Lowe*

Contribution from the Department of Chemistry, 152 Davey Laboratory, The Pennsylvania State University, University Park, Pennsylvania 16802. *Received September 13, 1985*

Abstract: Extended-Huckel band calculations for five patterns of ordered overlayers of hydrogen atoms on unreconstructed graphite (11% coverage) show energy differences as large as ~15 kcal mol^{-1}. These energy differences are primarily due to differences in interactions between the H atoms and graphite and not direct interactions between H atoms. The results of the band calculations are, to some degree, in accord with predictions based on the frontier crystal orbitals of graphite, though there are significant differences. Embedded cluster calculations on these systems yield the same frontier orbitals as band calculations, hence the same qualitative predictions, *only when cluster size meets a certain modular requirement.* This prevents smooth convergence with increasing cluster size. As a result, embedded-cluster frontier-orbital predictions of relative pattern stabilities get worse for these systems when one goes from an 18-carbon cluster to a 32-carbon cluster.

When atoms or molecules chemisorb on clean, crystalline surfaces, they sometimes form ordered overlayers, even at coverages of a small fraction of a monolayer.[1-3] At such low coverages, distances between adspecies can be too large for direct

0002-7863/86/1508-2527$01.50/0

(steric) interactions to be responsible for significant energy differences between various patterns of equal coverage. Therefore indirect, through substrate, interactions must be considered. In this paper we employ extended-Huckel theory (EHT)[4,5] to examine the system of hydrogen atoms chemisorbed atop carbon atoms on the basal plane of graphite (11% coverage) and address the following questions:

1. What are the relative energies of five different patterns as calculated from band theory?
2. Can these results be understood in terms of frontier crystal orbitals?
3. How well do cluster calculations, especially using embedded clusters, agree with band calculations of relative pattern stabilities, and how does this agreement depend upon cluster size?

Theoretical Model

Our reason for choosing graphite is that it is a quasi-two-dimensional crystal, allowing us to ignore all planes below the surface without seriously affecting the results of the calculations.[6] Also, d orbitals are not involved. We choose hydrogen atoms as adsorbate because of computational simplicity (only one AO per atom), reliability (EHT treats carbon–hydrogen bonding reasonably accurately), and size (small atoms minimize steric effects). We choose to place the hydrogen atoms directly over the carbon atoms (the "atop" position) because the preponderance of earlier theoretical studies indicates this position to be lower in energy, for hydrogen, than over a bond or over the center of a hexagon.[7] All hydrogens are placed 0.110 nm above the graphite plane. The EHT method is used because it is relatively inexpensive, can distinguish between various patterns of chemisorption, and expresses total energy as a sum of orbital energies—a feature we need if we are to evaluate effects of individual orbitals.

There is interest in the nature of the interactions between hydrogen and graphite, especially in connection with the mechanism for graphite corrosion by H_2 at high temperatures.[8] This process may involve chemisorbed hydrogen atoms, but there is, as yet, no experimental observation of ordered overlayers of atomic hydrogen on graphite: *We are interested in this system primarily as a model.*

Band Calculations

Method. The practical details of computing the energy bands for a periodic system are well-known. We employ a program devised by Whangbo and Hoffmann that produces the extended-Huckel crystal orbitals (EHCOs) and their energies for a given choice of unit cell and wavevector k.[9] Running the program for a series of k values within the first Brillouin zone (FBZ) allows one to plot the energies vs. k to produce band diagrams. We obtain the energy per unit cell (EPUC) for a system by integrating the band energies (times occupation numbers) over the k range in the FBZ using the numerical integration method of Chadi and Cohen.[10] Relative stabilities of isomeric ordered structures result

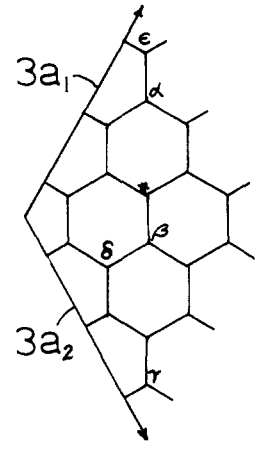

Figure 1. Unique sites for a second chemisorbed hydrogen atom in an 18-carbon-atom unit cell if the first hydrogen is chemisorbed over the position marked with an asterisk. a_1 and a_2 are unit translations of the *primitive* lattice. (See Figure 3a.)

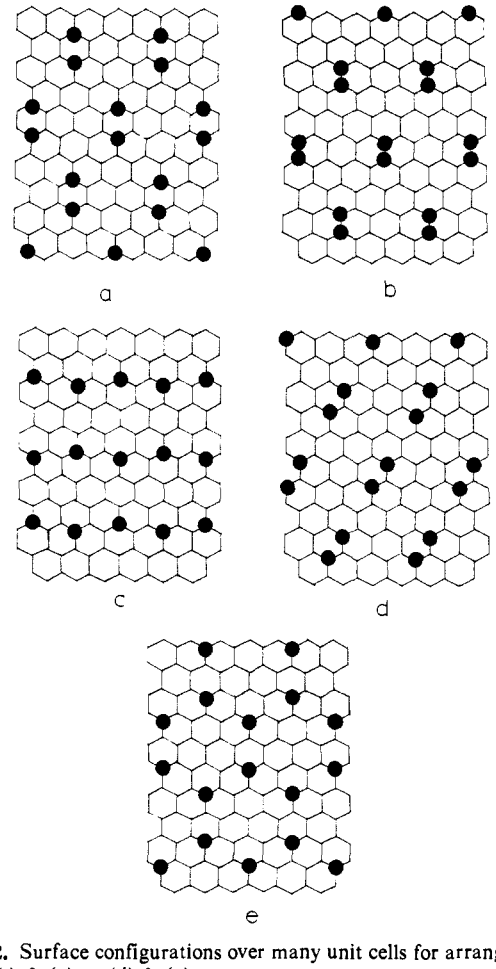

Figure 2. Surface configurations over many unit cells for arrangements (a) α, (b) β, (c) γ, (d) δ, (e) ϵ.

(1) Tong, S. Y. *Phys. Today* **1984**, *37*(8), 50–59.
(2) Somorjai, G. A.; Szalkowski, F. J. *J. Chem. Phys.* **1971**, *54*, 389–399.
(3) Muskat, J. P. *Surf. Sci.* **1981**, *110*, 85–110.
(4) Hoffmann, R. *J. Chem. Phys.* **1963**, *39*, 1397–1412.
(5) Hoffmann, R.; Lipscomb, W. N. *J. Chem. Phys.* **1962**, *37*, 2872–2883.
(6) Burdett, J. K.; Lin, J-H. Acta Crystallogr., *Sect. B: Struct. Crystallogr. Cryst. Chem. 38*, 408–415.
(7) (a) Cohen, N. V.; Gordon, M.; Weissmann, M. *Solid State Commun.* **1976**, *20*, 219–223. (b) Cohen, N. V.; Gordon, M.; Weissmann, M. *Solid State Commun.* **1977**, *22*, 181–184. (c) Nishida, M. *Phys. Status Solidi B* **1980**, *97*, K133–K137. (d) Evarestov, R. A.; Lovchikov, V. A. *Phys. Satus Solidi B* **1977**, *79*, 743–751. (e) Bennett, A. J.; McCarroll B.; Messmer, R. P. *Surf. Sci.* **1971**, *24*, 191–208. (f) Bennett, A. J.; McCarroll, B.; Messmer, R. P. *Phys. Rev. B: Solid State* **1971**, *3*, 1397–1406. (g) Messmer, R. P.; McCarroll, B.; Singal, C. M. *J. Vac. Sci. Technol.* **1972**, *9*, 891–894. (h) Messmer, R. P.; Bennett, A. J. *Phys. Rev. B: Solid State* **1972**, *6*, 633–638. (i) Johnson, K. H.; Messmer, R. P. *J. Vac. Sci. Technol.* **1974**, *11*, 236–242. (j) Dovesi, R.; Pisani, C.; Ricca, F.; Roetti, C. *J. Chem. Phys.* **1976**, *65*, 3075–3084. (k) Dovesi, R.; Pisani, C.; Ricca, F.; Roetti, C. *J. Chem. Phys.* **1976**, *65*, 4116–4120. (l) Dovesi, R.; Pisani, C.; Ricca, F.; Roetti, C. *Surf. Sci.* **1978**, *72*, 140–156. (m) Dovesi, R.; Pisani, C.; Roetti, C. *Surf. Sci.* **1981**, *81*, 498–502. (n) Ricart, J. M.; Illas, F.; Dovesi, R.; Pisani, C.; Roetti, C. *Chem. Phys. Lett.* **1984**, *108*, 593–596. (o) Ricart, J. M.; Virgili, J.; Illas, F. *Surf. Sci.* **1984**, *147*, 413–426. (p) Caballol, R.; Igual, J.; Illas, F.; Rubio, J. *Surf. Sci.* **1985**, *149*, 621–629. (q) Anganoa, G.; Koutecky, J.; Pisani, C. *Surf. Sci.* **1982**, *122*, 355–370. (r) Casanas, J.; Illas, F.; Sanz, F.; Virgili, J. *Surf. Sci.* **1983**, *133*, 29–37.
(8) (a) Balooch, M.; Olander, D. R. *J. Chem. Phys.* **1975**, *63*, 4772–4786. (b) Sen, A.; Bercaw, J. E. *J. Phys. Chem.* **1980**, *84*, 465–466. (c) Rosner, D. I.; Allendorf, H. D. *Heterogeneous Kinetics at Elevated Temperatures*; Belton, G. R., Worrell, W. L., Eds.; Plenum: New York, 1970; pp 231–251.
(9) Whangbo, M. H.; Hoffmann, R.; Woodward, R. B. *Proc. R. Soc. London A* **1979**, *366*, 23–46.
(10) (a) Chadi, D. J.; Cohen, M. L. *Phys. Rev. B: Solid State* **1973**, *7*, 692–699. (b) Chadi, D. J.; Cohen, M. L. *Phys. Rev. B: Solid State* **1973**, *8*, 5747–5753.

Table I. Relative Energies per Unit Cell for Five Ordered Overlayers of Hydrogen Atoms on Graphite

case	EPUC, eV	case	EPUC, eV
α	0.0	δ	0.470
β	0.170	ϵ	0.590
γ	0.307		

from comparing their EPUC values.

Choice of Unit Cell. If we wish to descibe a low-coverage ordered overlayer, we must select a unit cell that itself exhibits low coverage. This requires that the graphite segment in the unit cell have enough carbon atoms so that we can place hydrogens atop a few of them and still have most of the carbon atoms uncovered. Figure 1 shows the segment of a graphite sheet that we have selected for the surface portion of the unit cells studied here. It contains 18 carbon atoms. When hydrogen atoms are placed atop two carbons, we have 11% coverage (ignoring nonatop possibilities). There are five unique choices we can make for pairs of atop positions for the hydrogen atoms, and these lead to the ordered overlayers sketched in Figure 2. It is convenient to place one hydrogen atom at the site marked with an asterisk in Figure 1. Then the unique spots for the other hydrogens can be taken to be the sites labeled α–ϵ.

These computations do not allow for effects of geometrical rearrangement about a carbon when it bonds to a hydrogen atom. This surface-reconstruction energy should be significant. Also, there are other 11% coverage patterns that could be considered. (On an infinite surface, there is an infinite number of them.) The cases we deal with are merely the unique ones resulting from our choice of a particular unit cell. Therefore, we cannot claim that the results of our calculations are an accurate or complete reckoning of 11% coverage of graphite by hydrogen atoms. However, the model serves our purpose—*the comparison of various methods for calculating the energies of ordered overlayers.*

Numerous workers have considered the question of which type of site (over atom, bond, or hexagon center) a chemisorbing atom or molecule will prefer? The manner in which relative site stabilities are affected by choice of theoretical method, cluster size, use of cluster vs. band methods, extent of surface coverage, and frontier orbital symmetry have all been examined. We emphasize that we are *not* addressing the question of relative *site* stability. Rather, we are considering the relative stabilities of different *patterns* of coverage for a *given type* of site and a fixed extent of coverage. We know of no earlier treatment of this question, although the work of Messmer and Bennett[7h] (to be discussed later) is closely related. The factors influencing relative site preference are quite different from those influencing relative pattern stability, in much the same way that different factors influence ethane's bond energies and lengths on the one hand and relative conformational energies on the other. In particular, relative pattern stability, like conformation, should be sensitive to orbital overlap, rather than electron repulsion, considerations.

Results. The EPUC for each of the five arrangements appears in Table I. The energy difference between the most stable case (α) and the least stable (ϵ) is calculated to be about 0.6 eV, or about 15 kcal mol^{-1}. This is a substantial energy difference, much too large to be attributed to changing steric interactions between hydrogen atoms separated as widely as in, for instance, cases γ and ϵ. (See Figure 2, parts c and e.) It must result from differences in π-electron localization energies inherent in the patterns.

Frontier Orbital Treatment

Frontier Orbitals in Solids. Fukui,[11] Woodward and Hoffmann,[12] and others[7h,13] have pointed out that the energetics of many reactions within or between finite molecules are dominated,

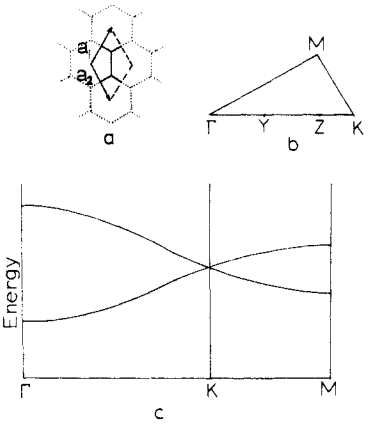

Figure 3. (a) Primitive unit cell for graphite and its translation vectors. (b) Reduced first Brillouin zone for graphite. Each point in the figure corresponds to a pair of wavenumbers that define the crystal orbitals. The reduced zone accounts for all unique crystal orbitals. (c) π-crystal orbital energy bands. Abscissa points are defined in (b).

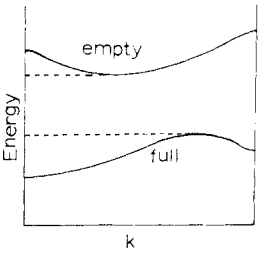

Figure 4. The energies of the highest HOMO and the lowest LUMO need not come at the same k value.

or at least paralleled, by the energy behavior of the frontier MOs and that it is possible to make qualitative predictions about frontier orbital energy behavior from perturbation arguments involving MO coefficient sizes and phases. We instituted this research with the goal of seeing whether a similar approach works for reactions involving an infinite surface. Specifically, does the energy order of Table I correlate with expectations based on the frontier crystal orbitals (FCOs) of graphite?

The frontier orbital concept requires further definition in cases of infinite periodic solids. Consider the π-band diagram of Figure 3c. The lower π-band is filled; the upper band is empty. There are σ-bands (not shown) above and below, but not between, these π-bands.[14] Hence, the π COs are the FCOs at any value of k. Since we have an infinite number of k values within the FBZ, we have an infinite number of sets of FCOs. While we can consider the natures of these FCOs at various k values, we are primarily interested in the highest of all the occupied and the lowest of all the unoccupied FCOs. These come at the point $k = K$ for graphite. In order to distinguish these FCOs from those at other k points, we refer to them as *leading* FCOs (LFCOs). Note that, in cases where a gap exists between valence and conduction bands, the LFCOs need not be associated with the same k value. (See Figure 4.)

Identifying the LFCOs. At the point K there are four half-filled, degenerate crystal orbitals.[7h] Because these orbitals are degenerate, there are countless ways they can be expressed. However, as soon as the graphite is perturbed by attachment of hydrogen atoms atop two of the carbons in a unit cell, the appropriate forms for some of the COs become specified. In the language of perturbation theory, there is a particular set of LFCOs that are appropriate zeroth-order functions for each of the perturbations we are concerned with. The general character of these "proper" LFCOs is as follows: Up to two members of each set have nonzero coefficients of equal absolute magnitude at the two sites of hy-

(11) (a) Fukui, K. *Science (Washington, D.C.)* **1982**, *218*, 747–754. (b) Fujimoto, H.; Fukui, S. A. *Chemical Reactivity and Reaction Paths*; Klopman, G., Ed.; Wiley: New York, 1974; pp 23–54.

(12) Woodward, R. B.; Hoffmann, R. *Angew. Chem., Int. Ed. Engl.* **1969**, *8*, 781–853.

(13) Pearson, R. G. *J. Am. Chem. Soc.* **1972**, *94*, 8287–8293.

(14) This statement applies to the more accurately computed band structures. The EHMO method predicts that the FCOs are σ-type in some k regions. However, these do not interact strongly with a hydrogen atom in the atop position.

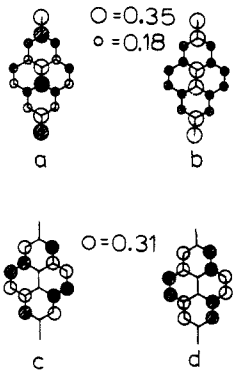

Figure 5. Correct zeroth-order leading frontier crystal orbitals for α, β, and γ patterns. Orbitals (c) and (d) retain freedom of mixing.

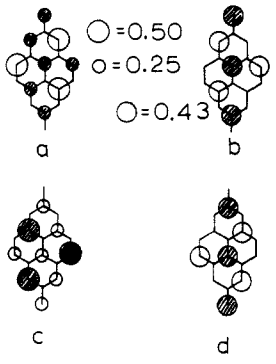

Figure 6. Correct zeroth-order leading frontier crystal orbitals for arrangement δ. Orbitals (c) and (d) retain freedom of mixing. All nonzero coefficients in (b) and (d) equal ±0.43. All those in (a) and (c) equal ±0.50 or ±0.25.

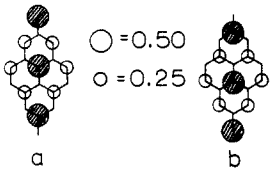

Figure 7. Two proper zeroth-order leading frontier orbitals for arrangement ϵ. The other two orbitals are the same as those in Figure 5, parts c and d.

drogen attachment. If there are two such COs in a set, the coefficients at these sites are of the same sign in only one case. All other COs in each set have coefficients of zero at both attachment sites. The proper LFCOs for cases α, β, and γ are identical and are sketched in Figure 5. For cases δ and ϵ, different CO sets apply, and these are shown in Figures 6 and 7, respectively.

Evaluating Relative Energies. Imagine that two hydrogen atoms bind to the graphite plane, one at the asterisked site, the other at one of the sites α, β, or γ. The appropriate (unnormalized) initial orbitals for the hydrogens are $(1s_1 \pm 1s_2)$, which are degenerate if we ignore interactions between the H atoms. Referring to Figure 5, we see that the antisymmetric H—H orbital can interact with CO 5a, the symmetric H—H orbital can interact with CO 5b, and COs 5c and 5d are unaffected, to first order. The CO energy lowering for each of the two perturbed levels is proportional to the CO coefficient, 0.35. Hence, the net effect is proportional to 0.70.

Turning to the δ case, we again find two proper LFCOs with the correct symmetry to interact with the hydrogens (Figure 6, parts a and b). In this case, the net effect is proportional (to first order) to 0.43 + 0.25 = 0.68. Hence, the first-order stabilization of the δ arrangement is predicted to be very slightly less than that for the α, β, and γ cases, according to the FCO at the point $k = K$.

The ϵ case has only one proper LFCO of symmetry appropriate for interaction with hydrogens (Figure 7a). The lowering of energy due to this CO is proportional to 0.50.

The result of this crude analysis, then, is that cases α–δ should have about the same stability and that case ϵ should be markedly less stable. This comes about because cases α–δ involve first-order interactions between two half-filled LFCOs and two half-filled hydrogen orbitals, while the ϵ case corresponds to interactions between one half-filled LFCO and one of the two half-filled hydrogen orbitals.

There are two kinds of "total" energy we can compare to the LFCO-based predictions. One of them is the sum of one-electron EHT energies at the same k value that gives these LFCOs, namely, K. These numbers, which contain *all* valence-electron energies, are listed in Table II. They are quite consistent with the FCO prediction except for case β, which is less stable than expected. The β case is the case of closest H—H approach, and it is possible that an antibonding interaction between hydrogens is preventing an even better agreement. (The Mulliken overlap population between hydrogens is −0.014 in the β case at k = K.)

The second "total" energy we can compare with is the EPUC, which we calculate by integrating total energies of the above type over all values of k in the Brillouin zone. These energies are displayed in Table I. We see that there is some agreement with Table II, in a qualitative sense, insofar as the energy *order* is concerned, but that the energy differences do not agree well with the FCO predictions. For instance, the energy difference in Table I between α and δ (which the LFCOs predict to have similar energies) is larger than that between δ and ϵ (whose energies are predicted to be different).

It is the comparison between LFCO predictions and EPUC that is most interesting in a practical sense. However, it is placing rather a tall order on the FCOs at one k point to describe quantitatively what accrues from summing over all COs and all k points. In view of this, the fact that the one pattern predicted to be least stable by the LFCOs actually turns out to be the least stable when we calculate the EPUC is encouraging. The patterns that are predicted by the LFCOs to have similar stabilities show substantial EPUC variations, reflecting the fact that they are predicted to have unequal stabilities at other k points. (See Figure 8).

The four degenerate LFCOs we have considered here become six COs when one considers a point on the k axis arbitrarily near, but not exactly at, the point $k = K$.[15] However, energy arguments based on the reduced set of four COs at K are representative of the regions in the vicinity of $k = K$. This is a general feature of symmetry arguments in MO theory, as Kertesz and Hoffmann have pointed out.[16]

Table II. Relative Total EHT Energies for Five Ordered Overlayers at the LFCO k Value

case	energy, eV	case	energy, eV
α	0.00	β	0.11
γ	0.00	ϵ	0.34
δ	0.08		

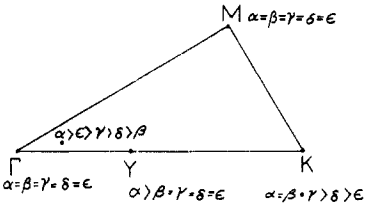

Figure 8. Predicted relative stabilities based on frontier crystal orbitals at various points in k space.

Cluster Calculations

Isolated Clusters. A common approach for computations on infinite solids or surfaces is to substitute a cluster thought to be sufficiently large to represent adequately the properties of in-

(15) Kleinman, L. *Phys. Rev. B: Solid State* **1974**, *9*, 1989–1992.
(16) Kertesz, M.; Hoffmann, R. *J. Solid State Chem.* **1984**, *54*, 313–319.

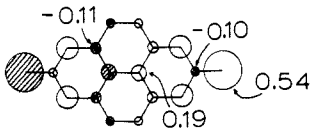

Figure 9. LUMO for an isolated 18-atom carbon cluster with no adsorbate.

Table III. Relative Energies for Two Hydrogen Atoms Bonded to an 18-Carbon-Atom Isolated Cluster

case	tot valence 1-e energy, eV	case	tot valence 1-e energy, eV
γ	0.00	δ	2.29
ϵ	0.18	α	2.60
β	2.06		

terest.[17] Sometimes the edges of the cluster are capped by atoms to saturate the dangling bonds that are absent in the infinite structure.[18] This can be partly accomplished for graphite by attaching hydrogens in the plane around the edge of a planar cluster of carbon atoms. While this removes the problem of dangling σ-bonds, it does not prevent the π-AOs on edge carbons from sensing an environment very different from that in graphite. The cluster is *isolated* as far as the π-system is concerned.

The results of an EHT calculation on an 18-carbon isolated cluster are summarized in Table III and Figure 9. There are now more than five unique hydrogen binding arrangements, but we restrict ourselves to the same α–ϵ cases. It is apparent that the calculated order of stabilities has changed. The preference for α and ϵ is simply a reflection of the fact that these two cases involve binding atop carbons that are very poorly linked to the cluster (bonded to only one other carbon) and hence have much residual bonding capacity. This shows up as large coefficients in the cluster frontier MOs (Figure 9). It is evident that *pattern* predictions based on *isolated* clusters would require careful design so that differential edge effects do not bias the results. (Note that this does not mean that cluster calculations are necessarily inappropriate for consideration of *individual site* preference.)

Embedded Clusters. A method has been devised[7h,19] for causing the edges of a cluster to sense a continuation of the periodic potential outside of the cluster. In effect, as usually applied, the method corresponds to carrying out an infinite structure calculation at only one point in k space. Ordinarily, this sample is taken at $k = 0$, though one can adjust this. If we select the 18-carbon cluster and adopt this procedure, we obtain the relative cluster energies of Table II, i.e., the same energies obtained from a normal band calculation at $k = K$. This results from the fact that, when we go from a 2-carbon to an 18-carbon unit cell for graphite, the band diagram goes from that shown in Figure 3 to a "folded-back" diagram. It happens that the folding associated with the 18-carbon unit cell brings the $k = K$ value back to $k' = 0$ in the folded diagram. Hence the embedded cluster method, in sampling the $k' = 0$ point for an 18-carbon unit cell, happens to be sampling the $k = K$ value in Figure 3c. The fact that cluster size affects the k point being sampled leads to the following peculiar result: Suppose we decide to use graphite FCOs as a basis for predicting relative pattern stabilities and choose to do an embedded cluster calculation to get the FCOs. Then, since choice of cluster size affects the amount of folding, and this in turn affects the k values that get folded back to $k' = 0$, we find that *the nature of the FCOs, and hence predictions based on them, varies nonmonotonically with cluster size.* In the present case, we find that we get the "correct" FCOs (i.e., the LFCOs) using an 18-carbon embedded cluster. Any multiple of the 18-carbon unit will give the same result. However, if we use a 32-carbon cluster (Figure 10 without

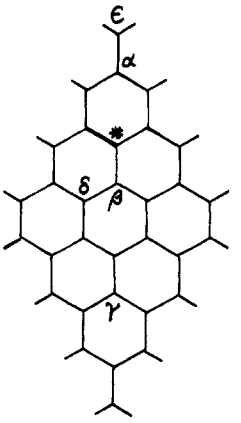

Figure 10. The 32-carbon-atom cluster with chemisorption sites marked. Edge carbons are bonded to hydrogens in the molecular plane.

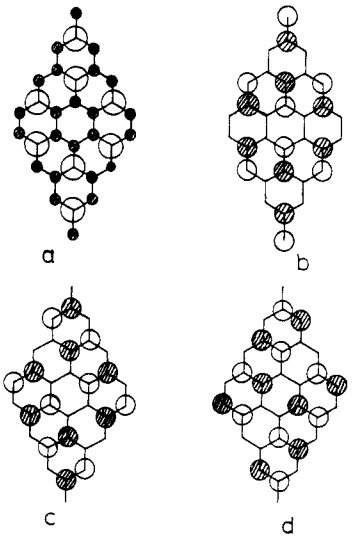

Figure 11. Correct zeroth-order frontier orbitals for a 32-atom embedded cluster: (a) α; (b) β and ϵ; (c) γ; (d) δ. In (a), all nonzero coefficients equal ± 0.42 or ± 0.14. In all other cases, they equal ± 0.34.

Table IV. Relative Energies for Two Hydrogen Atoms Bonded to a 32-Atom Embedded Cluster of 2s Atomic Orbitals

case	tot 1-e energy, eV	case	tot 1-e energy, eV
α	0.00	β	2.01
γ	1.74	ϵ	2.15
δ	1.74		

hydrogens attached) we get FCOs shown in Figure 11, corresponding to the point labeled Y in Figure 8, and we would predict from these that β–ϵ are similar in energy and that α is more stable. This is borne out by s-orbital-only calculations[20] on the 32-atom embedded clusters with two hydrogens attached. (These calculations correspond to only about 6% coverage, about half-way to the structures we have been considering, but should be representative of the relative energy order that would be predicted at 11% coverage.) The relative sums of one-electron energies for these cases, shown in Table IV, illustrate again the correspondence between the prediction based on FCOs of graphite and the actual EHT energies at the corresponding k value. The trouble is the 32-carbon cluster yields FCOs that do not correspond to the LFCO k value and hence are not likely to agree with the relative stabilities obtained by integrating over all k values. In short, a larger

(17) Upton, R. H.; Goddard, W. A., III *CRC Crit. Rev. Solid State State Mater. Sci.* **1981**, *10*, 261–296.
(18) (a) Zhidomirov, G. M. *Kinet. Catal. (Engl. Transl.)* **1977**, *18*, 977–984. (b) Mikheiken, I. D.; Abronin, I. B.; Zhidomirov, G. M.; Kazansky, V. B. *J. Mol. Catal.* **1978**, *3*, 435–442. (c) Hayns, M. R. *Theoret. Chim. Acta* **1975**, *39*, 61–74. (d) Vervoerd, W. S. *Surf. Sci.* **1981**, *108*, 153–168.
(19) Zunger, A. *Phys. Rev. B: Solid State* **1978**, *17*, 626–641.

(20) The full valence set of AOs for a 32-carbon-atom cluster exceeds our program's dimensions. Replacement of each carbon by a hydrogen whose 1s AO has the same exponent and valence-state ionization potential as a carbon 2p AO yields the results of Table IV and Figure 11.

embedded cluster does not necessarily give better FCO-based predictions.

Relation to Earlier Work

Messmer and Bennett,[7h] in a seminal paper, examined the FCOs of graphite in an attempt to establish symmetry rules for chemisorption *site* preference. Because they used an 18-carbon-atom embedded cluster to generate the FCOs, they based their arguments on the LFCOs. (Use of a different cluster size would have led to other, presumably less dominating, FCOs, a fact that Messmer and Bennett recognized but did not emphasize.) They examined the phases of the LFCOs and, by relating these to phases of MOs of various types of adsorbing species, proposed rules for predicting which sites (atop, over a bond, etc.) would be favored. Clearly, the philosophy behind that work is similar to our effort to relate pattern preference to the nature of the LFCOs. Indeed, Messmer and Bennett allude to this pattern question as a possible extension of their method.[7h] Their results, like ours, are necessarily approximate because they are predicting the results of integrating over all of k space from symmetry arguments at one point. It is also necessary, in both types of study, to mix the degenerate LFCOs of graphite to produce the proper zeroth-order COs for the perturbation analysis. Messmer and Bennett omitted this step.[19] This has the effect of preventing the theoretical surface from responding fully to the shifting about of the chemisorbing species, leading to an artificial enhancement in the predicted stabilities of some sites over others and to incorrect site-preference predictions. Despite criticism of their paper,[19] it contains an idea of some importance—that LFCOs in surfaces can be used to make qualitative predictions concerning chemisorption.

Conclusions

The frontier orbital hypothesis, that the relative total electronic energies for a series of related situations are paralleled by the relative frontier orbital energies, works well for hydrogen atoms on graphite *at each point in k space*. However, we have to integrate over all k points in the first Brillouin zone to obtain the energy per unit cell. This results in relative energies that are not well represented by any particular frontier crystal orbital. Nevertheless, the prediction based on the *leading* frontier orbitals—that the ϵ pattern should be less stable than all the others—is true for the energies per unit cell. Therefore, this one point in k space appears to be the most reasonable choice to represent (imperfectly) the integrated results.

Embedded-cluster calculations produce crystal orbital energies at only one k point. Since it is apparently best if that k point corresponds to the *leading* frontier crystal orbitals, it is important that the embedded-cluster size corresponded to a folded band structure wherein the desired k point has ended up at the origin of the k vectors.

Simple cluster calculations are inappropriate *for the sort of pattern comparisons considered here*. It is probably much easier to use an embedded cluster or band calculation than to attempt to adjust the shape and size of a simple cluster to overcome inherent deficiencies.

Registry No. H, 12385-13-6; graphite, 7782-42-5.

Surface Structure of Coadsorbed Benzene and Carbon Monoxide on the Rhodium(111) Single Crystal Analyzed with Low-Energy Electron Diffraction Intensities

M. A. Van Hove,* R. F. Lin,† and G. A. Somorjai

Contribution from the Materials and Molecular Research Division, Lawrence Berkeley Laboratory, and Department of Chemistry, University of California, Berkeley, California 94720.
Received August 26, 1985

Abstract: The first structural analysis of a molecular coadsorbate system is presented. Mutual reordering and site shifting are found to occur for benzene and CO coadsorbed in a $\begin{pmatrix}3&1\\1&3\end{pmatrix}$ lattice on Rh(111). This low-energy electron diffraction (LEED) intensity analysis yields the first confirmed hollow-site adsorption of CO on a single-crystal metal surface, with a C–O bond length expanded by 0.06 ± 0.05 Å from the gas phase. The flat-lying benzene is found centered over hcp-type hollow sites with a strong Kekulē-type distortion: C–C bond lengths alternate between 1.33 ± 0.15 and 1.81 ± 0.15 Å (hydrogen positions were not determined). This suggests the possibility of a 1,3,5-cyclohexatriene species being formed. The Rh–C bond length is 2.35 ± 0.05 Å for benzene and 2.16 ± 0.04 Å for CO.

1. Introduction

A growing amount of structural information is becoming available on monolayers of aromatic molecules adsorbed on transition-metal surfaces.[1] The main techniques used to obtain such information are high-resolution electron energy loss spectroscopy (HREELS), low-energy electron diffraction (LEED), thermal desorption spectroscopy (TDS), angle-resolved ultraviolet photoemission spectroscopy (ARUPS), and near-edge X-ray absorption fine structure (NEXAFS). We report here on the structure of benzene adsorbed on the Rh(111) single-crystal surface in the presence of coadsorbed carbon monoxide. LEED intensity analysis and HREELS were the primary techniques used in this study. This is the first structure analysis of a two-molecule adsorption system to yield detailed information on the bonding of both molecules to the metal. The interaction between these coadsorbates shows up both in ordering and in bonding effects: the long-range order depends on the relative coverage (concen-

† Permanent address: Department of Physics, Fudan University, Shanghai, People's Republic of China.

(1) (a) Nyberg, G. L.; Richardson, N. V. *Surf. Sci.* **1979**, *85*, 335. (b) Tsai, M.-C.; Muetterties, E. L. *J. Phys. Chem.* **1982**, *86*, 5067. (c) Massardier, J.; Tardy, B.; Abon, M.; Bertolini, J. C. *Surf. Sci.* **1983**, *126*, 154. (d) Surman, M.; Bare, S. R.; Hofmann, P.; King, D. A. *Surf. Sci.* **1983**, *126*, 349. (e) Avery, N. R. *Surf. Sci.* **1984**, *146*, 363. (f) Koel, B. E.; Crowell, J. E.; Mate, C. M.; Somorjai, G. A. *J. Phys. Chem.* **1984**, *88*, 1988. (g) Newmann, M.; Mack, J. U.; Bertel, E.; Netzer, F. P. *Surf. Sci.* **1985**, *155*, 629.

0002-7863/86/1508-2532$01.50/0